Draft 20 December 2000

Accuracy of Modelled Stratospheric Temperatures in the Winter Arctic Vortex from Infra Red Montgolfier Long Duration Balloon Measurements

J.-P. Pommereau[1], A. Garnier[1], B.M. Knudsen[2], G. Letrenne[3], M. Durand[3], P. Cseresnjes[1], M. Nunes-Pinharanda[1], L. Denis[1], A. Hauchecorne[1] and P. A. Newman[4]

1. Service d'Aéronomie, CNRS, Verrières le Buisson, France

2. Danish Meteorological Institute, Copenhagen, Denmark

3. Centre National d'Etudes Spatiales, Toulouse, France

4. NASA Goddard Space Flight Center, Greenbelt, USA

To be submitted to *J. Geophys. Res.*

Short title: Evaluation of modelled temperature in the winter stratosphere

Abstract.

The temperature of the stratosphere has been measured in the Arctic vortex every 9-10 minutes along the trajectory of four Infra Red Montgolfier long duration balloons flown for 7 to 22 days during the winters of 1997 and 1999. From a number of comparisons to independent sensors, the accuracy of the measurements is demonstrated to be ± 0.5 K during nighttime and at altitude below 28 km (10 hPa). The performances of the analyses of global meteorological models, ECMWF 31 and 50 levels, UKMO, DAO, NCEP and NCEP/NCAR reanalysis, used in photochemical simulations of ozone destruction and interpretation of satellite data, are evaluated by comparison to this large (3500 data points) and homogeneous experimental data set. Most of models, except ECMWF31 in 1999, do show a small average warm bias of between 0 and 1.6 K, with deviations particularly large, up to 20 K at high altitude (5hPa) in stratospheric warming conditions in 1999. Particularly wrong was ECMWF 31 levels near its top level at 10 hPa in 1999 where temperature 25 K colder than the real atmosphere were reported. The average dispersion between models and measurements varies from ± 1.0 to ± 3.0 K depending on the model and the year. It is shown to be the result of three contributions. The largest is a long wave modulation likely caused by the displacement of the temperature field in the analyses compared to real atmosphere. The second is the overestimation of the vertical gradient of temperature particularly in warming conditions, which explains the increase of dispersion from 1997 to 1999. Unexpectedly, the third and smallest (± 0.6-0.7 K) is the contribution of meso and subgrid scale vertical and horizontal features associated to the vertical propagation of orographic or gravity waves. Compared to other models, the newly available ECMWF 50 levels version assimilating the high vertical resolution radiances of the space borne Advanced Microwave Sounding Unit, performs significantly better (0.03 ± 1.12 K on average between 10 and 140 hPa in 1999) than other models.

1. Introduction

Large ozone reductions have been reported in the 90's in the Arctic polar stratospheric vortex in the winter qualitatively consistent with heterogeneous activation of chlorine on polar stratospheric clouds (PSC) forming at low temperature. Though qualitatively generally consistent with observations, its amplitude if often underestimated by photochemical 3D CTM (Chemical Transport Models) particularly when the temperature is close to that of formation of PSCs *[Goutail et al. 1999, Goutail et al., 2000, Guirlet et al., 2000, Lefèvre et al., 1998; Deniel et al., 1998, Chipperfield, 1999]*. Among uncertainties suggested to explain the underestimation, one the most sensitive is that of the temperature in the analyses of meteorological models used to prescribe photochemical simulations. Indeed, and in contrast to Antarctica where the temperature is persistently well below that of PSC formation throughout the winter, the average temperature in the winter Arctic stratosphere is close to that of formation of PSC type Ia (NAT). It drops below that of type II ice particles condensation episodically only. The presence of PSC is thus limited in time and geographic extension. Therefore, small errors or systematic biases in the temperature in the meteorological analyses could lead to large errors in the predicted ozone loss in this highly non linear system. In addition, meso-scale processes such as gravity or orographic waves not or partially captured only by global models of limited grid size, could result in local cooling events of large amplitude where PSC could form *[Carlslaw et al., 1998, Leutbecher and Volkert, 1996, Dörnback et al., 1998]*. Though orographic coolings are known to occur sporadically, their climatology and therefore their global influence on ozone destruction, is little known.

Testing the ability of a meteorological model to capture stratospheric temperature and wind at global and meso-scales is not straightforward. Most of available radiosonde data are already

included in the initialisation or assimilation scheme of the models. In addition, they are also of limited number in the Arctic winter for various reasons: i) reduced number of stations, recently dropped by a factor four in Russia for economical reasons; ii) burst of balloons at low temperature at the tropopause or little above; iii) high wind speed, which makes the balloon to be out of telemetry range when reaching the stratosphere. On the other hand, the comparison between various models with each other [e.g. *Manney et al., 1996*] highlights differences but does not allow to decide which is better. Several studies have been carried out for evaluating the quality of the temperature and wind of analyses of the different models, using a variety of methods. TOVS satellite retrieved temperatures have been used by *Swinbank and O'Neill [1994]* to evaluate the United Kingdom Meteorological Office (UKMO) data assimilation model, also compared to radiososondes by *Manney et al. [1996]*. Radiosondes of the network have been also used and compared to the ECMWF analyses or first guess field (the six hour forecast from the previous analysis) assumed to be independent from errors on individual radiosondes *[Knudsen 1996a]*. Finally, *Pullen and Jones [1997]* have been using the data set of 28 ozonesonde stations only partially included in the network and available during the winter of 1994/95 during the European campaign SESAME, for evaluating UKMO analyses.

Alternatively the data from the few available long duration balloons flights have been also used to carry such studies. Temperature and wind velocity measured along 1-6 day trajectories of 8 ballast controlled balloons conducted in 1992-95 within the Polar Vortex Balloon Experiment (POVORBEX) of the University of Wyoming, have been compared to analysis of the European Centre for Medium Range Weather Forecasts (ECMWF) *[Knudsen et al., 1996b]*. Past NASA and CNES long duration balloons at a variety of latitudes have also been used for evaluating wind analyses and forecast in the mid-stratosphere by the UKMO and DAO assimilation systems *[Keil et al., 1999]*. Finally, *Knudsen et al. [2000]* have investigated

the quality of wind analyses of a variety of models in the Arctic vortex from the trajectories of the balloons described in this paper.

From these studies and regarding temperature, it has been often concluded that a systematic positive bias (analyses warmer than the atmosphere) existed in the models in the middle stratosphere in the winter over the Arctic, particularly at low temperature. Its amplitude in the UKMO model has been estimated to 1.3 to 3.7 K at T < 200K, reduced to 0.6 K if all temperature are considered, by *Manney et al., [1996]* or up to 1.7 K on average at low temperature (NAT point) by *Pullen and Jones [1997]).* Though of lesser amplitude, a bias of 0.6 to 1.7 K at T < 200K has been also reported in the model of NMC (US National Meteorological Center), however of less than -0.2 if all temperatures are considered *[Manney et al., 1996].* A systematic average positive bias of 2.0 K at 30 hPa was also found in ECMWF in the winter 1994-95 north of 60°N and of 1.8K at 50 hPa in January 1996 *[Knudsen et al., 1996a].* However, the bias in ECMWF seems to have dropped after January 1996 when ECMWF moved from an optimum interpolation procedure to a 3-dimensional variational scheme allowing to better combine the radiosondes and the low resolution TOVS temperature data from the NOAA satellites *[Knudsen et al., 1996a].*

Another constant feature resulting from the above studies, is the relatively large standard deviation, of 2-3 K depending on the model, in the difference between analyses and individual sondes and increasing with altitude *[e.g. ,Manney et al., 1996, Pullen and Jones 1997].* This scatter is generally attributed by the authors to small scale vertical structures in the temperature profiles and likely also to mesoscale orographic waves not captured by a model of limited truncature and number of height levels.

Here we report on an experimental evaluation of the temperature of a variety of models (ECMWF, UKMO, DAO, NCEP and its NCAR reanalyses) in the winter Arctic stratospheric

vortex from a series of data obtained from four long duration Montgolfier Infra-Red (MIR) balloon flights carried out in 1997 and in 1999. The duration of the flights (12 and 22 days in 1997, 7 and 17 days in 1999) during which the temperature is sampled every 9^{th} minutes (97) or 10^{th} minutes (99) and the vertical excursion of the balloons allow to investigate possible altitude dependent biases as well the cause of the dispersion.

Though the balloons were carrying several other instruments for measuring ozone, NO_2, CH_4, H_2O and aerosols, here we will concentrate on meteorological measurements only. But since this is the first time MIR balloons are flown in the polar vortex, we will present first the experimental set-up and the performances of the measurements.

The paper is organised in two sections. The first is a description of the experiment and the flights followed by an in depth discussion of the accuracy of the meteorological measurements, a prerequisite for looking at possible biases in the models. The second includes, after a short description of the models, the comparison of modelled and actual temperatures in 1997 and 1999 and an analysis of the amplitude of the various terms contributing to observed differences: altitude and temperature dependencies, long wave and mesoscale contributions.

2. Long duration balloon flights and meteorological measurements

2.1 The Infra-Red Montgolfier system

The balloon is a hot air Infra-Red Montgolfier (MIR) developed by the CNES Balloon Division following an idea suggested by *Pommereau and Hauchecorne (1979)*. It carried a total payload of 50/70 kg depending on the arrangement, made of two independent packages separated by 30/50 m: a service gondola (SAMBA) of 22 kg hosting meteorological and balloon control measurements as well as cut down sub-systems, and a scientific payload of 20/40 kg depending on the flight (**Fig. 1**). The scientific payload could be either a uv-visible SAOZ spectrometer for measuring ozone and NO_2 on both flights in 1997, or a combination of a SAOZ, a tunable diode laser for measuring CH_4 in situ and a Lyman alpha hyrgometer on the first flight of 1999, or an in situ ozone semi-conductor sensor and a backscatter diode laser for measuring PSCs in the second flight. A description of those instruments and preliminary results could be found in *Pommereau and Piquard [1994], Pommereau et al. [1997], Garnier et al. [1999], Denis et al. [1999], Gardiner et al. [1999] and Yushkov et al. [1999]*. Each gondola had its own temperature, pressure and location measurements by Global Positioning System (GPS) and an ARGOS transmitter for satellite data collection and Doppler location. For air traffic safety reasons, the flights were limited to the inside of the vortex and automatically terminated if the balloon was flying south of 55°N or below 140 hPa (13.5 km geometric altitude in the vortex, 14.5 km standard aircraft flight level). All balloons have been launched from ESRANGE, the facility of the Swedish Space Corporation at Kiruna in Northern Sweden, who was also controlling the flights. Clearance was obtained from Air Traffic Control (ATC) and defence authorities of all countries north of 55°N. A complementary control station run by the Central Aerological Observatory of Moscow was also set at Murmansk for controlling the flights above Russia.

2. 1. 1. IR Montgolfier

The MIR is a hot air balloon of 45 000 m^3 volume in aluminised Mylar (IR absorbent Mylar inside, aluminium of low IR emissivity outside) for its upper part and IR transparent polyethylene for the bottom. It is heated by the thermal emission of the earth and the atmosphere only during night-time and additionally by the sun during the day. Though more than 40 flights have been carried out in the tropics *[Malaterre et al., 1996]*, it has never been flown in the polar winter. But, since the lift of the balloon at night is directly proportional to the difference between the brightness temperature of the surface flown over and air temperature at flight level, it is particularly adapted to the cold winter vortex. Indeed in those conditions the atmospheric temperature at 20 km is of the order of -80°C and that of the ground or clouds is always warmer than -50°, -60°C even in the coldest part of the Arctic (Siberia, Greenland or North pole). This is more than enough to ensure a difference of 15°-25°C between the gas and the outside and to allow the balloon to stabilise between 18 and 22 km (60-40 hPa) at night. During daytime, additional solar heating makes the balloon to ascend to higher levels, typically around 25-27 km (15 hPa) depending on albedo and sun zenith angle. But since this arrangement does not allow the MIR to leave the ground by itself, an initial lift is provided by helium which result in a higher flight level during the first day, at 34 km (4-5 hPa). After two days, the helium is totally evacuated and the balloon reaches its normal hot air flight level.

The main limitation of the system is the occurrence of warm temperature that happens during a stratospheric warming, between February and April depending on the year. If the temperature of the atmosphere at flight level warms up to –50 / -60°C, the difference with the brightness temperature of the surface below could become too small in some cases (e.g. above high and dense clouds, the Greenlandic ice cap or mountain ranges in Siberia), and the balloon could drop to altitudes where it must be cut-down. We will see later that some significant

altitude drops did indeed occur and in one case, with the heavier payload, resulted in the termination of the flight.

2. 1. 2. SAMBA service gondola

The role of the SAMBA (Système d'Acquisition de Mesures en BAllon) gondola is threefold. It allows the monitoring of the flight (altitude, location, temperature and pressure and IR global flux in 1999). It activates the cut-down, the strobe-light and the radar transponder requested by Air Traffic Control (ATC) if the balloon is flying below 140 hPa or south of 55°N. Alternatively, it terminates the flight after a given duration to allow the recovery of the payload. The data are transmitted to the ground through the ARGOS satellite data collection system but there is no control from the ground. All systems are run automatically.

Location is provided by both GPS (Global Positionning System, Trimble Navigation) and ARGOS (Doppler shift). Two Honeywell sensors of different ranges measure pressure: 0-1000 hPa for the ascent sensor and 0-145 hPa of 1 hPa accuracy for the float sensor. They are both temperature compensated. Ambient temperature is measured by two Veco aluminised micro-thermistors of 250 μm diameter mounted on 1 m long booms deployed a little after launch on each side on the gondola. The thermistors are calibrated in a cold chamber between 170K and 320K, with an accuracy of ± 0.5K given by the manufacturer of the chamber. All parameters are sampled regularly every 9 minutes (10 minutes in 99). The ARGOS system is particularly efficient at high latitude since 26 to 28 satellite overpass can be expected per day, though it is still limited at 120 kbits /day at best.

Two cut down systems made of independent actuators and pyrotechnic knives are used in parallel. A pressure sensor mechanically actuates the first if the balloon is reaching 140 hPa.

An on-board CPU actuates the second from information given by the GPS, if south of 55°N or if the geometric altitude is lower than 13.5 km (aircraft standard level of 14.5 km or 48 kft) or after a given maximum duration fixed before the flight. Termination is commanded following two modes. First, the detection system is activated after x days, but cut down occurs only when the balloon is reaching a pre-determined area where recovery is possible (Scandinavia or European Russia). Second, the flight is terminated in all cases after (x + 8) days, the absolute limit defined by the power capacity of the lithium batteries. Since it was the first time such flight was attempted in the winter in polar areas, x was set at 12 days for the first balloon in 1997 and 20 days for the others.

The total weight of the SAMBA payload, including lithium batteries, is 22 kg for a maximum autonomy of about 30 days.

2. 1.3. Meteorological measurements onboard the scientific gondola

In addition to instruments measuring ozone, chemicals or tracers, the scientific payload carries also a set of meteorological sensors: pressure, temperature and location / altitude by GPS of Trimble Navigation. Meteorological sensors are those of a Vaïsala RS-80 radiosonde [temperature of 0.2°C (1 s.d.) repeatability and 2.5 s time constant; pressure of 0.5 hPa (1 s.d.) repeatability according to the manufacturer]. Capacitive measurements relative to a reference capacitor and temperature compensation are handled by the standard Vaïsala ground software installed permanently into the on-board CPU. Calibrations are those of the manufacturer updated in the on-board CPU and adjusted by comparison with the measurements of a meteorological station prior to launch, following the recommendations of the manufacturer. For the first flight in 1997, the sensors were mounted on the side of the

gondola as for short duration balloon flights. But since this arrangement proved to be noisy at float at constant level, a 1m long boom was added for the following flights.

The scientific gondola has its own ARGOS transmitter and is powered by lithium batteries only. For power saving, the number of measurements is limited to a hundred per day. The CPU and all the sub-systems, but the transmitter and its memory, are switched off and awaked by a micro-controller when needed only. Since the main objective is to measure profiles by solar occultation at sunset and sunrise or during the descent / ascent of the balloon, the 100 data points are not equally distributed during the day. Most of them are concentrated during twilight. Otherwise during day and night, the measurements are limited to one reading every 1.5 hours. The temperature and pressure sampling of the scientific gondola is thus limited.

2. 1. 4. Flight train and additional radiosonde

The flight train of the two balloons flown in 1997 and distances between the various elements are shown in figure 1. The SAMBA gondola bearing pressure, temperature and location measurements is hanging 8 m below the bottom of the balloon and the scientific payload 46 m below. An additional autonomous Vaisala RS-80 radiosonde of limited lifetime (3h) was attached at the bottom of the flight train for consistency checks of pressure and temperature during the initial night-time ascent. The total weight carried by the balloon was of 46 kg.

The experiments flown in 1999 were a little different. The first was carrying the same SAMBA service payload but a more complex and heavier scientific payload for a total of 71kg. The second was carrying a SAMBA payload only onto which the ozone and PSC sensors were hosted and thus the total weight was reduced to 45 kg. Both flights were carrying also the additional radiosonde active during the first 3 hours.

The arrangement, list of scientific instruments, weight and flight information are summarised **in table 1**.

2. 2 Balloon flights

Because of the automatic cut down of the balloon south of 55° N and also the need for low temperature for the MIR to fly efficiently, it was decided that the launch could take place in the vortex only. In addition, since solar occultation measurements as well as daytime ascent of the balloon require some sun, it was decided not launch prior the 15th of February. Four flights have been carried out : two in 1997 and two more in 1999.

2. 2. 1. 1997 flights

The vortex was exceptionally strong, cold and long lasting in 1997 since it did not break before mid April [*Coy et al., 1997, Naujokat et al. 1997*]. **Figure 2** shows PV and temperature maps at 475K isentropic level calculated from ECMWF analyses at the beginning, the middle and the end of the flights. The location of the balloon on that day is shown by a cross. In 1997, the vortex remained almost circular and centred around the pole until spring with a temperature pattern very similar, the minimum temperature being co-located with the centre of the vortex.

The first launch opportunity occurred on February 24th when the vortex drifted above the station. The balloon trajectory, its altitude, atmospheric temperature, PV at and orography 475K at the location of the balloon location, are displayed in **figure 3.** PV is compared to the inner and outer edges of the vortex calculated following to the method suggested by *Nash et al. [1996]*. Since the sampling period is of 9 min and the average speed of the balloon of 24 m/s, the measurements were repeated every 13 km on average.

The launch took place in the evening so as to reach float at 34 km before sunrise. The flight lasted for 12 calendar days (16 flight days and 17 nights) until March 9th when probably an erroneous cut-down order was delivered by the CPU above Greenland, although it should have waited for flying over Scandinavia for being actuated. The balloon remained inside the vortex at almost constant PV at latitude higher than 60°N during its three turns around the pole. After one and a half day and the loss of additional helium, the daytime flight level became stable at about 25-26 km (13-18 hPa). During night-time, it varies from 20-22 km (30-45 hPa) at cold temperature (-75°, -80°C) to 14.5 km geometric altitude (108 hPa) at two occasions at warmer temperature (-65°) above the Baffin sea and southern Greenland.

The second attempt took place on the March 17th. The balloon was launched at the inner edge of the vortex. It lasted in flight for 22 calendar days (26 flight days, 27 nights) until its automatic cut down above Scandinavia after 5 turns around the pole. The instrument landed safely on April 8th near Trondheim in Norway where it was recovered on the following day. The trajectory and altitude of the balloon, air temperature, PV at 475 K and ground altitude are displayed in the right panels of **figure 3**. On average the daytime altitude was a little higher (26-26 km) than during the first attempt because of the higher sun and therefore the larger contribution of albedo during daytime. In contrast, the night-time altitude was lower, often around 17 km, because of the warmer stratosphere. The trajectory was almost circular and fast (38 m/s on average), excepted at the end of the flight when the balloon drifted to the inner edge of the weakening vortex.

The SAMBA gondola performed well, excepted the unexpected cut-down after 12 days, although there was no reason clearly identified for that. All meteorological sensors performed well throughout the flight.

Figure 4 (top) shows the evolution of the temperature measured at night during both flights from February 24th until April 4th and at bottom the altitude profile. On average, the lower stratosphere was observed to warm up progressively from 193 K to 215 K during the period with a sharp altitude minimum shifting from 30 hPa at beginning of the period to 50-60 hPa at the end. The temperature remained relatively homogeneous in the vortex. The amplitude of the temperature modulation between one side and the other of the vortex did not exceeded 10 K.

2.2.2. 1999 flights

Totally different was the meteorology of 1999 when the vortex was already weak and relatively warm in mid-February and warmed up and split rapidly in early March *[Naujokat, 2000]*. **Figure 5** shows the evolution of the vortex and the temperature field at 475 K of the ECMWF analyses et beginning, middle and end of the flights. By mid-February, the vortex was already elongated with a cold centre on the European side and warmer air on its Siberian side. It split in two parts in late February which moved to rapidly to mid latitudes. A warm anticyclonic area developed over the pole and the circulation reversed (easterlies) at the end of February.

Since the forecast was not promising, it was decided to launch the two balloons close together on two successive days, on the 18th and 19th of February. **Figure 6** shows the trajectory and altitude of the balloons, air temperature, PV at 475K and the altitude of the ground below the balloon. After a fast turn into the small vortex, the second being a little deeper inside, the two balloons drifted slowly toward Eastern Siberia in a warm stratosphere area over a cold mountain range. The first was cut down after 7 days calendar over the Siberian mountain range when reaching its minimum permitted altitude immediately before

sunrise on the 24th of February. A model of flight adjusted on observed parameters has shown that the balloon would have survived with a payload of 60 kg instead of 71 kg *[Garnier et al., 1999]*. Since these conditions were the worst, which could be expected in the Northern Hemisphere, 60 kg appears a reasonable weight for a 45 000m^3 volume MIR to survive in all conditions in the winter vortex. The lighter second flight survived and returned backward to Scandinavia and Canada when the wind direction reversed in the Arctic after the warming of the stratosphere. It was automatically cut-down when reaching the latitude of 55°N off the Labrador coast when the vortex vanished on the 8th of March after 17 days of flight where it was lost.

Among meteorological sensors, three incidents have been reported:

i) One temperature failed (T1) in the first flight since the boom did not deployed correctly. It will not be further used.

ii) Both temperatures in flight 2 were found shifted by the same amount (approx. + 3K) compared to the ascent radiosonde, to the temperature of the scientific gondola as well as to independent radiosondes when flying around Yakutsk. The reason for that is that the thermistors flown were not that calibrated together with the SAMBA electronics recovered after an unfortunate previous launch attempt during which the thermistors were broken. The onboard conversion algorithm was therefore wrong. Since the difference was found identical for both thermistors and consistent with three independent data sets, a quadratic correction was calculated and applied uniformly to both sensors.

iii) The Honeywell float pressure sensor of MIR 2 drifted by some 10 hPa within 17 days probably because of a leak in the sensor, which did not appeared during the tests at ground. Since the measurements cannot be reliably corrected, they have been replaced by ECMWF

pressure at altitude measured by the GPS of ± 100 m accuracy as described in Knudsen et al. [2000].

Figure 7 shows the evolution of the night-time temperature recorded during both flights and its altitude profile. The altitude of the temperature minimum was unusually high (20 hPa) at the beginning of the flights with a steep gradient above. During the next two weeks, the warming shifted rapidly downwards to end up with a minimum temperature at 80 hPa by the end of the period. The steep gradient is the cause of the large temperature drop at the beginning of each night after day 54 during the descent of the balloon in the upper panel.

2. 3 Accuracy of meteorological measurements

Since the objective is to compare meteorological data recorded on-board the balloons to models, the accuracy of the measurements needs to be carefully assessed.

GPS location and geometric altitude transmitted by the two independent gondolas of ± 100 m accuracy according to the manufacturer, were indeed always found consistent with each other within the specification. The GPS location was always found also consistent with the ARGOS Doppler readings though the latter are less precise (between 500 m to 3 km depending on the viewing angle of the satellite), and the altitude with the geopotential height of the radiosonde. There is therefore no reason for questioning the accuracy of location and altitude of ± 100 m given by the GPS manufacturer.

In contrast, pressure readings are found much less accurate than anticipated. An average bias of up to –2 hPa is reported between Honeywell and Vaisala sensors, and in addition there is a systematic difference of 2-3% between readings during the morning ascent and the evening descent compared to pressure calculated from GPS latitude. This is indicative of a hysteresis in the Honeywell pressure sensors, usually vibrated in short duration balloon flights but not here

because of power limitation. On average, and ignoring the leak of the sensor of MIR 99 # 2 already indicated, the accuracy of the sensors is of ± 2 hPa with a repeatability of ± 1hPa.

Temperature measurements are difficult on balloons at float because of the drop of forced convection compared to IR and solar heating, perturbation when in the wake of the gondola, Joule heating of the thermistor, and in the case of ARGOS, transmission errors. An idea about the precision could be obtained by comparing the simultaneous measurements of the two thermistors at opposite sides of the gondola. In turns, the accuracy could be checked by three independent methods, all related to radiosondes: i) comparison with the additional radiosonde during the initial ascent; ii) comparison along the flight with the low sampling rate Vaisala Thermocap on-board the scientific payload, and iii) comparison with the radiosondes of the GTS network when the balloon is passing close to an upper air station.

2. 3. 1. Comparison between T1 and T2 on-board the same gondola

The two thermistors T1 and T2 on the SAMBA payload are in principle identical and their measurements independent and simultaneous. The comparison of their readings along the flights offers then a good indicator of the precision and repeatability of the measurements. **Figure 8a** shows the difference between T1 and T2 during the 17 days of the MIR 2 flight in 1999. On average, T1 is warmer by 0.39 K but the difference also shows a large dispersion of ± 1.97 K (1 s.d.). **Figure 8b** shows the same data plotted vs SZA (Sun Zenith Angle). It is obvious that the measurements are more dispersed during daytime. If the data set is split into day and night (SZA>93°, approximately the moment of sunset when the balloon starts to descend rapidly in the evening), the difference becomes 0.29 ± 2.97 K during daytime and 0.46 ± 0.30 K at night.

The measurements are 8 times more dispersed during the day. They are largely perturbed at high altitude around 15 hPa when in the wake of the slowly rotating gondola when the thermistors are alternatively passing in the lee of the payload. Indeed the aluminised skin of the gondola is strongly heated by the sun (more than 100°C above ambiant). Ideally the themistors should be mounted far from the payload. But the risk is then to break them during launch operations. Perhaps the best would be to have both systems in the flight train. Meanwhile, for the above reason, all daytime measurements will be ignored in the following. Note that the criteria of SZA>93° implies that descent data in the evening will be kept but not that of the morning ascent after sunrise by definition since it is the result of solar heating.

Another aspect of the noise of the measurements is the altitude dependence of the dispersion of the night-time data shown in **figure 8c**. The dispersion of the difference increases with altitude because of the drop of convection. Even at night at 3.4 hPa during the first 24h of flight and at 15 hPa on the second day, temperature measurements are difficult. If the two first nights are ignored, the average dispersion at pressure larger than 20 hPa drops to ± 0.30 K. Similar analyses have been conducted for all flights, the results of which are summarised in **table 2**. On average, at night and below the 20 hPa level (26 km), the dispersion of temperature measurements is of the order of ± 0.4 K which includes thermal perturbation as well a telemetry errors since the ARGOS system is not free of such errors.

2. 3.2. Comparison to additional radiosonde during initial ascent

As already said, a RS-80 radiosonde was added to the flight train for comparison during the first night-time ascent. For three hours, the sampling rate of the two thermistors of the SAMBA gondola was also accelerated to 1/ 50s transmitted to an ARGOS ground receiver when still in the telemetry range. As an example, the difference between T2 and the reading of

the Vaisala Thermocap sensor of flight #1 in 1999 is shown in **figure 9**. The picture is typical to what is observed on all flights: i) a significant systematic bias of about 1K in the steep tropospheric temperature gradient due to the difference of time constant between the pressure and GPS altitude sensors; ii) an almost constant difference with relatively little dispersion (± 0.21 K in present case) in the small stratospheric temperature gradient up to 28-30 km (10 hPa); iii) an increasing difference and a larger dispersion above when the sensors are much less ventilated (large Thermocap sensor warmer than thermistors).

2. 3. 3. Comparison to low sampling rate SAOZ Vaisala Thermocap

Though of faster sampling rate, thermistor measurements could be also compared to those of the Vaïsala Thermocap sensor of the scientific payload throughout the whole night in 1997 but at twilight only in 1999. As an example, **figure 10** shows the difference between night-time T1 and T_{SAOZ} during the 22 day flight of MIR#2 in 1997. On average, the difference is of + 0.15 ± 0.61 K. Similar results have been obtained on MIR#1 in 97 but more dispersed (0.39 ± 2.3 K) because of the bad mounting of the SAOZ sensor too close from the gondola. Similar also is the figure for MIR#2 in 99 (0.55 ± 1.2 K) but still dispersed in that case because twilight measurements were available only on the SAOZ payload. There was no independent scientific gondola on MIR#2 in 99.

2. 3. 4. Comparison to radiosondes of the network

The MIR temperature readings have been also compared to the closest radiosonde data when the balloon is passing near a station of the network. Selected stations from which full ascents data have been obtained are: Sodankyla in Finland, Thule and Scoresbysund in

Greenland, Ny-Alesund in Svalbard and Yakutsk in Eastern Siberia. However, co-locations are infrequent and in addition the altitude range of overlap is limited because of the burst of the radiosonde balloon. Thirteen data points have been obtained only for the two flights of 1997 together within a distance of 1500 km. Though the dispersion is quite large (-0.04 ± 2.58 K), no significant departure appears between the two sets of data and more important, no sign of temporal drift. If the distance is restricted to 500 km the number of co-locations drops to 5 but the result (0.87 ± 2.07 K) is very similar. A better comparison was reached in 99 with the radiosondes of Yakutsk, when the two MIRs were travelling around the station for 2-3 days. **Figure 11** shows the comparison of the Russian radiosonde at Yakutsk on the 26th of February 1999 and the MIR measurements. In the altitude range of 13-18 km where they do overlap (most of soundings at Yakutsk stop at 18 km), the difference does not exceed 0.6 ± 0.5 K. The figure for the first MIR (0.3 ± 0.6 K) is very similar.

2. 3. 5. Summary of temperature accuracy

The information available from all previous comparisons is summarised in **table 3.** Overall, it can be concluded that, night-time temperature measurements at levels below 28 km (10 hPa) are consistent to within the ± 0.5 K accuracy given by the sondes manufacturers and calibrations in the laboratory. On average, the dispersion of the measurements in flight is of the order of ± 0.4 K. However, these figures degrades above 28 km where an accuracy of ± 2 K only would be more appropriate, though the error could be due also to the radiosonde itself.

2. 4 Concluding remarks

Four MIR have been successfully flown in the Arctic vortex in the winter demonstrating that this type of vehicle is well adapted to this use even during a stratospheric warming event, providing the total weight of the payload does not exceed 60 kg for a volume of 45 000 m^3. It appears that the most difficult constraint to accommodate is the limitation of 55°N since the vortex frequently extends to this latitude in the Northern Hemisphere. An option could be to launch the balloon deeper in the vortex but this will require launch operations to be conducted at higher latitude, since the site of ESRANGE is infrequently located in the middle of the vortex.

A variety of meteorological measurements has been conducted along the flights. GPS location and altitude are found to be accurate within the specification of ± 100 m of the manufacturer. The accuracy of pressure measurements is little worse than expected (± 2 hPa) largely because of the time constant of the sensors. One pressure sensor completely failed but could be satisfactorily replaced by the conversion of GPS altitude into pressure using a meteorological model. Temperature was demonstrated to be measured with an average precision of ± 0.4 K and an average accuracy of ± 0.5 K, but during night-time and at altitude below 28 km only. Daytime temperature measurements are less reliable because of the thermal perturbation when in the wake of the gondola. Improvement would require temperature sensors far from other equipment but in turns risky to launch. Measurements at high altitude at float, even at night, are much more difficult. No satisfactory design has been suggested up to now. In the following, night-time temperature data will be used only.

3. Evaluation of temperature in numerical prediction models

Temperatures recorded during the four MIR flights in the winter Arctic vortex, have been compared to those of a variety of models in use in photochemical simulations of ozone loss. The analyses evaluated are: ECMWF (European Centre for Medium Weather Forecasts), UKMO (United Kingdom Meteorological Office), DAO (Data Assimilation Office) of NASA, NCEP (National Climatic Prediction Centre) and REA (NCEP/ NCAR reanalysis).

3.1. Description of the models

ECMWF analyses available in 1997 were those of the 31 level 3D variational data assimilation model in operation since January 1996 (see *Knudsen et al., 2000*). The number of vertical layers is 31 from the ground to 10 hPa, (near 10, 30, 50, 70, 90, 110 and 130 hPa in the stratosphere). The data used are those of six hourly analysis of T106 truncation corresponding to a 1.125° latitude-longitude grid. For 1999, two versions of ECMWF are co-existing: the same 31 levels version but augmented since November 1997 to a 4-D assimilation scheme, available at the time of the balloon flights, and pre-operational runs of the new 50 levels version, available later in May 1999. This new version extends to 0.1 hPa with a level spacing of about 1.5 km throughout the stratosphere. The 50 levels version, called later ECMWF50, includes for the first time the assimilation of the high vertical resolution radiances of the space borne Advance Microwave Sounding Unit (AMSU) [*ECMWF, 1999*].

UKMO is the UK Meteorological Office stratospheric data assimilation system using the Analysis Correction scheme in which observations are gradually inserted [*Swinbank and O'Neill, 1994*]. The model has 42 levels up to 0.28 hPa and a horizontal resolution of 2.5°

latitude by 3.75° longitude. The data used in this study are those produced for the Upper Air Research Satellite (UARS) project. The analyses are interpolated to the 22 UARS standard pressure levels (10, 15, 22, 32, 46, 68 100 and 147 hPa levels in this study). Note that the UKMO vertical resolution is better above 30 hPa than that of the ECMWF31 operational model and NCEP described below. The analyses are available at 12 UT only.

The DAO (data assimilation office) at GSFC produces stratospheric data assimilation analyses with 2° latitude by 2.5° longitude resolution (GEOS1). The observations are gradually inserted using the incremental analyses update scheme [*Schubert et al., 1993*]. The model has 46 levels up to 0.4 hPa of which 10, 30, 50, 70, 100, and 150 hPa are use here. The analyses are produced every 6 hours.

The NCEP model of the US Climate Prediction Centre provides temperature and geopotential heights on pressure surfaces from 70 to 0.4 hPa on a 65 x 65 polar stereographic grid interpolated to 5° longitude by 2° latitude. The levels used here are 10, 30, 50, 70, 100 and 150 hPa. The analyses are calculated by the successive correction method and include radiosondes and SSU satellite data. At 100 hPa and below the analyses are those of the T126 Global Data Acquisition System model. The NCEP analyses are available at 12 UT only (see *Knudsen et al 2000*).

The NCEP/NCAR reanalyses are available since 1956 [*Kalnay et al., 1996*]. They are produced from the same model as the NCEP analyses except that derived satellite temperatures are used instead of raw radiances. The analyses are made in 2.5° latitude-longitude grid and have X? levels up to 10 hPa of which 10, 30, 50, 70, 100, and 150 hPa are used here. They are available for every 6 hours.

In the following, all fields are interpolated in space and time by a linear procedure (log-linearly in pressure).

3. 2 Biases

The altitude dependence of the difference between modelled and actual temperatures for all flights in 1997 and 1999 are displayed in **figures 12 and 13**. The corresponding average differences and standard deviations calculated between 10 and 150 hPa are shown **in table 4**. Except for ECMWF, the features are very similar from one year to the other, but the amplitude of the dispersion, much larger in 1999. All models do show a more or less significant but always positive average bias varying from 0.03 K (ECMWF50 in 1997) to 1.54 K (DAO 1999) and 1.60 K (NCEP 1999). The bias is larger during the stratospheric warming period of 1999 than in the stable winter of 1997 but it is also altitude dependent. It increases at higher altitude in the mid-stratosphere. UKMO, DAO and REAN do show a positive bias of 3-5 K around 10-15 hPa in 1997 and 1999 as well as NCEP in the second year. The difference increases to 20 K at 5 hPa in 1999 though these figures could not be generalised since they correspond to a single day at the beginning of the flights as explained earlier.

In contrast, the difference with ECMWF31 varies from 1997 to 99. The bias is insignificant in 97 but of up to –20 K near the top of the model near 10 hPa. These low temperatures in the middle stratosphere were a permanent feature of ECMWF analyses and forecast during the winter of 1999. Often the model was predicting unrealistic temperatures lower than 173 K. This could be due to the coarse vertical resolution of satellite based temperatures which could easily give a wrong temperature at 10 hPa, when the coldest temperatures are at 20 hPa. It must be recalled also that the 97 and 99 versions of ECMWF31 are different, the first being using a 3-D variational assimilation scheme and the second a 4-D. Compared to this, the pre-operational ECMWF50 shows no bias even at high altitude in contrast to all other models.

3.3 Dispersion

The average dispersion in each case is summarised in **table 4.** Except for NCEP, it is generally larger in 99 than in 97. UKMO shows the smallest of ± 1.40 K in 97, while NCEP is the best operational model (± 1.80K) in 99. The dispersion of 1.12 K of the new ECMWF50 in 99 is significantly better than that of the other models on the same year.

The various causes of dispersion could be identified in the time series shown in **figures 14 and 15**. The relatively larger dispersion of DAO, REA and UKMO in 1999 is largely due a stronger vertical gradient of temperature which can be seen during the descent of the balloon at the beginning of each night on the three models but of smaller amplitude in NCEP and ECMWF31 and 50. The first three models overestimate the temperature gradient that is the warming of the stratosphere from above. Another contribution, which can be easily seen on both years, is the long wavelength signal of ± 2-3 K amplitude. In contrast to the previous, it is larger in NCEP and REA than in UKMO, ECMWF31 and DAO and even smaller in ECMWF50. But though often in phase between models (e.g. in 1997), it could be also in opposite phase (e.g. NCEP and REA in 99). In order to investigate if a systematic temperature dependence (e.g. model warmer or colder where it's warm or cold) could be responsible for that, a correlation study has been performed. **Table 5** shows the slope of the regression line between the difference of temperature and the temperature for the various models. The correlation is generally significant. The largest is the negative one in REA in 1999, which could be easily seen on figure 15. Therefore the long wave signal seems to be more related to horizontal displacements in the temperature field (e.g. larger or displaced vortex) than to a systematic amplification or reduction of temperature.

Another contribution suspected in the past to be the main reason for the dispersion in the difference between models and actual temperature, is the impact of vertical features of small

scale compared to the coarse vertical resolution of the models or caused by the upward propagation of orographic or gravity waves of horizontal scale small than their horizontal grid.. **Figures 16 and 17** show the dispersion of the difference between ECMWF31 in 97 or ECMWF50 in 1999 and MIR temperatures in reference to the average calculated for each night. Since the horizontal displacement of the MIR is most of the time larger than the grid of the models (up to 1500 km in 1997 during a single night) and the vertical excursion covers several model layers, it provides a good estimate of the impact of sub-grid scale features. The average amplitude of the 1 s.d. dispersion compared to the low vertical resolution ECMWF31 varies from ± 1.16 K during the first flight of 1997 to ± 0.93 K in the second in 1997. It does not significantly improve (± 0.97 K on average) in 1999 in ECMWF50 even though the spacing between levels is reduced to 1.5 kilometres. Though cases of lee waves of ± 2.5 K amplitude have been positively identified above the Ural or the Siberian mountain ridge associated to fast surface west wind [*Pommereau et al., 1999*], all attempts to correlate statistically the variance to orography failed. Since the dispersion of the measurements themselves was demonstrated to be at least of the order of ± 0.4 K, the contribution of small scale horizontal and vertical features and vertical gradient errors do not exceed 0.8 – 0.9K on average if a quadratic summation is assumed. This figure is consistent with the drop of dispersion from 1.2 K to 0.7 K after day 56 in figure 17, when the balloon was returning to the Northern Atlantic in easterlies when gravity waves cannot propagate upwards.

3.4 Concluding Remarks

For the first time, a large (1617 points in 1997 and 1861 in 1999) and homogeneous data set of temperature measurements spanning over a broad altitude range from 10 to 140 hPa was collected in the winter Arctic vortex. When compared to this, meteorological models do

always show a positive bias, small and little significant in stable vortex conditions as in 1997, but of larger amplitude in stratospheric warming conditions, where all models, UKMO, DAO, NCEP and NCEP/NCAR reanalysis, except ECMWF50, overestimate the vertical gradient of temperature. In those conditions, the ECMWF 31 levels 4-D variational scheme did particularly wrong near its top level of 10 hPa in 1999 where it frequently generated temperature 25 K below that measured.

The difference between modelled and measured temperatures do show a dispersion of 1.4 - 2.0 K in 1997 increasing to 1.8 – 3.0 K in 1999, except again ECMWF50 which displays a dispersion of ± 1.1 K only in 1999. The largest contribution to the dispersion is due to a long wave modulation of the difference likely caused by a horizontal displacement or deformation of the analysed temperature field compared to the reality. Most of the increase in dispersion from 1997 to 1999, results from an overestimation of the steep temperature gradient in stratospheric warming condition. Though suggested in the past to be the major cause of dispersion, meso- and small scale features in the horizontal and vertical temperature field, contribute for a relatively small part (0.8-0.9 K).

The new 50 levels version of ECMWF is found to perform better than all other models in both bias, vertical gradient and displacement of horizontal field. But although the vertical spacing between levels has been largely reduced in the stratosphere, the small scale dispersion do not improve significantly compared to the older 31 levels version. Most of the improvement in temperature as well in wind as suggested by Knudsen et al. *[2000]*, in addition to the higher top level, could likely result from the assimilation of the high vertical resolution of radiances of the Advanced Microwave Sounding Unit (AMSU).

Acknowledgements. The authors thank Pierre François and Eric d'Almeida for their hard work in building the SAOZ gondola, the CNES balloon division who designed and operated the SAMBA payload and the IR Montgolfier, Vaisala OY for providing the software of the radiosondes, the Swedish Space Corporation for the flights control, ATCs of all Arctic countries for authorising the long duration flights to take place, CAO for flight control over Russia, ECMWF, UKMO, NASA and NCEP for providing the results of their models, the radiosonde stations for providing their row data, and E.R. Nash for vortex edge calculations. The project was supported by the French Programme of Atmospheric Chemistry (PNCA), the Centre National d'Etudes Spatiales (CNES) and the DG Research of the European Commission (Lagrangian Experiment contract ENV4CT970504).

References

Carlslaw, K.S., M. Wirth, A. Tsias, B.P. Luo, A. Dörnback, M. Leutbecher, H. Volkert, W. Renger, J.T. Bacmeister, E. Reimer and T.H Peter, Increased stratospheric ozone depletion due to mountain-induced atmospheric waves, *Nature*, 675-678, 1998.

Chipperfield, M. P., Multiannual simulations with a three-dimensional chemical transport model, J. Geophys. Res., 104, 1781-1805, 1999.

Coy, L., E.R. Nash and P. A. Newman, Meteorology of the polar vortex: Spring 1997, *Geophys. Res. Lett*, 24, 2693-2696, 1997.

Deniel, C., R.M. Bevilacqua, J. P. Pommereau and F. Lefevre, Arctic chemical ozone depletion in the lower stratosphere during the 1994-95 winter deduced from POAM II satellite observations and the Reprobus 3-D model, *J. Geophys. Research*, 103, 19231-19244, 1998.

Denis. L., J. P. Pommereau, F. Lefèvre, F. Goutail, B. Knudsen and G. Letrenne, Ozone loss and NO2 recovery during the winter and spring 1997 as observed from long duration

balloons flights in the vortex, *Proc.5th European Ozone Symp.*, 425-428, EC Air Poll. Res. Report 73, 2000.

Dörnback, A, M. Leutbecher, H. Volkert and M. Wirth, Mesoscale forecasts of stratospheric mountain waves, Metor. Appl, 5, 117-126, 1998.

ECMWF *Newsletter*, No 83, Reading, UK

Gardiner, T., I. Howeison, G. Hansford, N. Swann, S. Garcelon, R.L. Jones and P. Woods, Measurements of Stratospheric Methane during THESEO using a Balloon-borne Near-Infrared Laser Absorption Spectrometer, *Proc.5th European Ozone Symp.*, 499-501, EC Air Pollution Res. Report 73, 2000.

Garnier, A, J. P. Pommereau, F. Nouel, V. Dubourg, G. Letrenne, Long duration balloon flights int he Arctic : The Lagrangian experiment, *Proc. 14th ESA Symp. on European Rocket and Balloon programmes*, ESA SP-437, 603-608, 1999.

Goutail, F. et al., Depletion of column ozone in the Arctic during the winters of 1993-94 and 1994-95, *J. Atm. Chem.*, 32, 1-34, 1999.

Goutail, F.,J. P. Pommereau and F. Lefèvre, Winter Ozone Loss in the Arctic and at mid-latitude in 1998 and 1999 from the SAOZ ground-based network and balloon measurements, *Proc. 5th European Ozone Symp.*, 433-436, EC Air Poll. Res. Report 73, 2000.

Guirlet, M., Chipperfield, M.P., Pyle, J.A., Goutail, F., Pommereau, J.P., von der Gathen, P. And Kyro, E., 1999, Modelled arctic ozone depletion in winter 1997/1998 and comparison to previous winters, *J. Geophys. Res.*, Vol. 105, D17, pages 22,185-22, 2000.

Kalnay, E., et al., The NCEP/NCAR 40-year reanalyses project, Bull. Am. Meteorol. Soc., 77, 437-471, 1996

Kiel et al., The use of long duration balloon data to determine the accuracy od stratosphere analyses and forecasts, J. Geophys. Res., in press, 2000.

Knudsen, B.M., Accuracy of arctic stratospheric temperature analyses and the implications for the prediction of polar stratospheric clouds, *Geophys. Res. Lett.*, 23, 3747-3750, 1996a.

Knudsen, B. M. et al., Comparison of analysed temperatures and calculated trajectories with long duration balloon data, *J. Geophys. Res.*, 101, 19, 137-145, 1996b.

Knudsen, B.M., J. P. Pommereau, A. Garnier, M. Nunez-Pinharanda, L. Denis, G. Letrenne, M. Durand and J.M. Rosen, Comparison of stratospheric air parcel trajectories based on different meteorological analyses, *J. Geophys. Res.*, in press, 2000.

Lefèvre, F., F. Figarol, K.S. Carslaw, and T.H. Peter, The 1997 Arctic ozone depletion quantified from three-dimensional model simulations, *Geophys. Res. Lett.*, 25, 2425-2428, 1998.

Letrenne, G., Compte-rendu des vols MIR en Arctique en 1997, CNES technical report, DOA/T/ED/BA/EP/08.30, 1998.

Leutbecher, M., and H. Volkert, Stratospheric anomalies and mountain waves : A three-dimensional simulation usinf a muti-scale weather prediction model, J. Geophys. Res., 23, 3329-3332, 1996.

Malaterre, P., V. Dubourg, G. Letrenne and M. Durand, The long duration MIR balloon, *Proc. 12th ESA Symp. on rocket and balloon programmes*, ESA SP-370, 329-334, 1996.

Manney, G.L, et al., Comparison of UK meteorological Office and U.S. National Meteorological Center stratospheric analyses during northern and southern winter, *J. Geophys. Res.*, 101, 10311-10334, 1996.

Nash, E.R., P. A. Newman, J. E. Rosenfield and M. R. Schoeberl, An objective determination of the polar vortex using Ertel's potential vorticity, *J. Geophys. Res.*, 101, 9471-9478, 1996.

Naujokat, B. and S. Pawson: The unusually cold, persistent vortex in spring 1997, Air Poll. Res. Rep 60, 50-53, 1998.

Naujokat, B., The winters of 1997/98 and 1998/99 in Perspective, *Proc. 5th European Ozone Symp.*, 107-110, EC Air Poll. Research Report 73, 2000.

Pommereau, J.P., and A. Hauchecorne, A new Atmospheric vehicle: The Infra-Red Montgolfier, *Adv. Space Res.*, 55, 1979.

Pommereau, J. P. and J. Piquard, Ozone, Nitrogen dioxide and Aerosol vertical distributions by UV-visible solar occultation from balloons, *Geophys. Res. Lett*, 21, 1227-1230, 1994.

Pommereau, J-P., L. Denis and F. Goutail, Study of the Arctic vortex using long duration ballons, Proc. *13th ESA Symp. on European Rocket and Balloon programmes*, ESA SP-397, 197-201, 1997.

Pommereau, J.P., P. Cseresnjes, L. Denis, A. Hauchecorne, G. Letrenne, B. Knudsen, Stratospheric temperature measurements in the winter Arctic vortex in 1997 on-board long

duration balloons : comparison to ECMWF model and detection of orographic waves, *Proc. Europ. Workshop on Mesoscale Porcesses in the Stratosphere*, Air Pollution Research Report 69, Carslaw and Amanatidis Ed., 211-216, 1999.

Pommereau, J.P., A. Garnier, F. Goutail, F. Vial, F. Nouel, V. Dubourg, G. Letrenne, R.L. Jones, G. Hansford, R. Freswater, K. Turnbull, K. K. Roscoe, D.E. Williams, P. Woods, T. Gardiner, A. Adriani, F. Cairo, V. Yushkov, S. Merkulov and B. Knudsen, Long duration balloon flights in the Arctic : the THESEO Lagrangian experiment, *Proc. 5th European Ozone Symp.*, 304-307, EC Air Poll. Res. Report 73, 2000.

Pommereau, J. P., A. Garnier, M. Nunez Pinharanda, L. Denis, B. Knudsen, F. Nouel, V. Dubourg and G. Letrenne, 1999, Evaluation of ECMWF stratospheric temperature in the polar vortex from long duration balloon measurements, *Proc. 5th European Ozone Symp.*, 570-573, EC Air Poll. Res. Report 73, 2000.

Pullen, S. and R.L. Jones, Accuracy of temperatures from UKMO analyses of 1994/95 in the arctic winter stratosphere, *Geophys. Res. Lett.*, 24, 845-848, 1997.

Rabier, F., H. Järvinen, E. Klinker, J.-F. Mahfouf and A. Simmons, The ECMWF operational implementation of four dimensional variation assimilation. I. Experimental results with simplified physics, *Q.J.R. Meteorological Soc.*, 126, 1143-1170, 2000.

Schubert, S.D., R.B. Rood, and J. Pfaendtner, An assimilated data set for Earth Science applications, Bull. Am. Meteorol. Soc., 74, 2331-2342, 1993

Swinbank, R., and A. O'Neill, A stratosphere-troposphere data assimilation system, *Mon. Weather Rev.*, 122, 686-702, 1994.

Yushkov, V., S. Merkoulov, V. Astakhov, J. P. Pommereau and A . Garnier, A Lyman alpha hygrometer for long duration IR Montgolfier during the THESEO Lagrangian Experiment, *Proc.5th European Ozone Symp.*, 404-407, EC Air Pollution Res. Report 73, 2000.

Flight	Instruments	Launch	Dur.	Weight	Cut down
97-1	P, T, GPS SAOZ O3 and NO2 profiles	24 Feb	12 d.	60 kg	Erroneous order
97.2	P, T, GPS SAOZ O3 and NO2 profiles	17 Mar	22 d.	60 kg	to enable recovery
99.1	P, T, GPS, Global IR radiometer SAOZ O3, NO2, OClO profiles TDL (CH4), H2O Lyman alpha	18 Feb	7 d.	71 kg	P> 140 hPa
99.2	P, T, GPS, Global IR radiometer Backscatter diode laser, O3 in-situ	19 Feb	17 d.	45 kg	Lat. < 55°N

Table 1. Summary of MIR flights in 1997 and 1999

	97.1	97.2	99.1	99.2
T1-T2 night	- 0.3 ± 0.9 K	+ 0.59 ± 0.43 K	NA	+ 0.46 ± 0.30 K

Table 2. Difference and standard deviation of nighttime and P>20 hPa simultaneous temperature measurements on-board the same gondola on 1m long booms 180° apart.

	97.1	97.2	99.1	99.2
T2 – asc. sonde	+ 0.01 ± 0.55	+ 0.32 ± 0.45	+ 0.01 ± 0.12	0.15 ± 0.25
T2 -Tsci	- 0.39 ± 2.30	- 0.15 ± 0.6	- 0.55 ± 1.20	NA
T2- network	-0.04 ± 2.6		+ 0.60 ± 0.5	0.3 ± 0.6

Table 3. Temperature difference and standard deviation between T2 on one hand, the ascent sonde, the scientific payload, and the sondes of the network on the other.

	ECMWF 31	UKMO	DAO	NCEP	REA	ECMWF50
1997	0.30 ± 1.45	0.42 ± 1.40	0.65 ± 1.74	0.06 ± 1.87	1.15 ± 2.03	NA
1999	0.59 ± 5.38	1.45 ± 2.48	1.54 ± 2.80	1.60 ± 1.80	1.33 ± 2.98	0.03 ± 1.12

Table 4. Average temperature difference (model-MIR) and standard deviation (P>10 hPa only).

	ECMWF 31	UKMO	DAO	NCEP	REA	ECMWF50
1997	-0.01± 0.006	0.02±0.006	0.01±0.007	0.07± 0.007	-0.012 ±0.007	NA
1999	0.31± 0.027	0.00±0.011	-0.03±0.012	0.03±0.008	-0.230 ±0.014	0.02 ± 0.005

Table 5. Slope of correlation line between difference of temperature and actual temperature

Figure Captions

Figure 1. Schematic of the IR Montgolfier system. The SAMBA service payload hanging 8 m below the bottom of the balloon, carries two temperature micro-thermistors mounted on 1 m long booms, 2 pressure sensors and a GPS. The scientific gondola 46 m below also carries pressure and temperature Vaisala sensors. An additional conventional RS-80 Vaisala radiosonde, but of 3h duration only, is added at the bottom for pressure and temperature consistency checks during the initial night-time ascent. Other sub-systems are from top to bottom: two independent cut-down mechanisms activated by a pressure sensor or by the CPU, a parachute, a radar transponder and a strobe light, all active during the initial ascent and final descent only and a radar reflector.

Figure 2. ECMWF Potential Vorticity and temperature fields at 475K at beginning (Feb 24th), middle (March 17th) and end (April 8th) of the balloon flights period in 1997. The cross represents the balloon location on that day.

Figure 3. Left : sixteen days (12 calendar days) trajectory, altitude, PV at 475 K, temperature and orography during the first flight starting at Kiruna on February 24th and ending over northern Greenland on March 7th (night-time solid line, daytime dotted). Right : same for the twenty six days (22 calendar days) second flight starting on March 17th at Kiruna and ending above the western coast of Norway on April 8th.

Figure 4. Time evolution (panel a) and vertical profile (panel b) of temperature measured at night by the balloons in Feb-April 1997. Though progressively warming from 195 to 215 K, the vortex remained relatively homogeneous during the 45 days. The amplitude of temperature change between the warm and cold sides of the vortex did not exceeded 10K. The altitude of the temperature minimum drifted slowly downward from 40 to 60 hPa.

Figure 5. ECMWF50 PV and temperature field at 475K and location of balloons at the beginning, middle and end of balloon flights in 1999. Already elongated in mid-February, the

vortex split into two pieces drifting rapidly towards mid-latitude in early March. By that time the warmer area was located over the pole and the circulation reversed.

Figure 6. Trajectory of balloons, altitude, air temperature, PV and orography in 1999 (Left MIR1; Right : MIR 2).

Figure 7. Same as figure 4 but for 1999. In contrast to 1997, the altitude of the temperature minimum shifted from an unusually high altitude (20 hPa) in mid-February to 50 hPa during the warming of the stratosphere by the end of February. The warming resulted in a steep temperature gradient which can be seen in the temperature measurements during the descent of the balloon in the evening of data after day 54 in the upper panel.

Figure 8. (a) Difference between temperature measured simultaneously on-board the same gondola by the two thermistors of MIR #2 in 1999; **(b)** Difference of temperature measured at P>10 hPa versus Solar Zenith Angle (SZA); **(c)** Altitude dependence of the dispersion of the nighttime temperature measurements.

Figure 9. Difference of temperature measured during the initial ascent by a thermistor (T2) and the radiosonde on MIR #2 1999.

Figure 10. Difference between temperature measured at night along the second MIR flight in 1997 by the thermistor (T2) and the Vaisala Thermocap sensor of the scientific gondola.

Figure 11. Comparison of MIR#1 T2 readings (dots) during the final descent of balloon on February 26th 1999 and the nearby radiosonde temperature report (line) at Yakutsk in Siberia.

Figure 12. Difference of temperature between model analyses and MIR temperature in 1997.

Figure 13. Same for 1999 (Note the increase of range of horizontal axis compared to figure 12.

Figure 14. Time evolution of the temperature difference (model-measurements) in 1997. Also shown in the lower panel is the temperature along the flights.

Figure 15. Same for 1999. The largest differences at the highest levels (fig. 13) do not fit into the plot.

Figure 16. Meso and small scale contribution in 1997. Panel (a): dispersion with respect to the average for each night; (b) daily average standard deviation; (c) orography along the balloon trajectory.

Figure 17. Same for 1999.

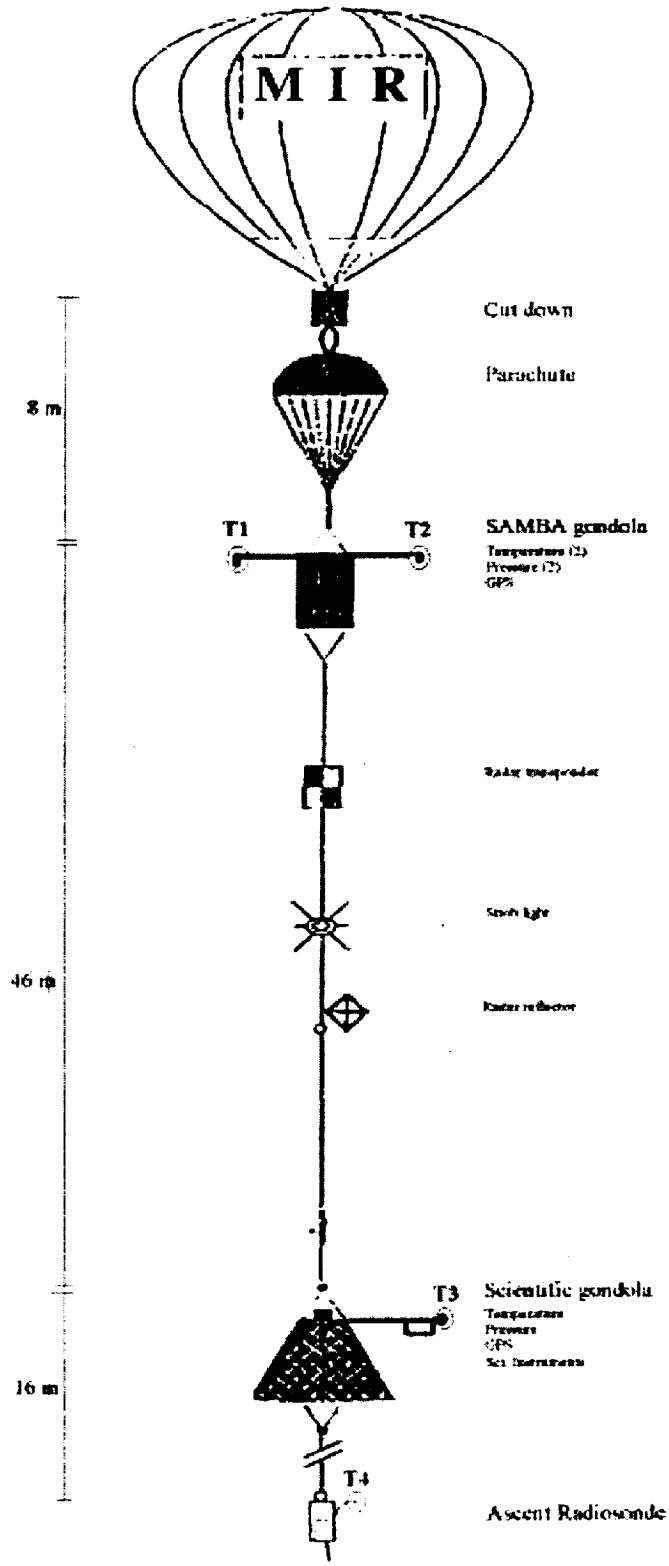
M I R
Cut down
Parachute
8 m
T1
T2
SAMBA gondola
46 m
T3
Scientific gondola
16 m
T4
Ascent Radiosonde

Figure 1.

Figure 2

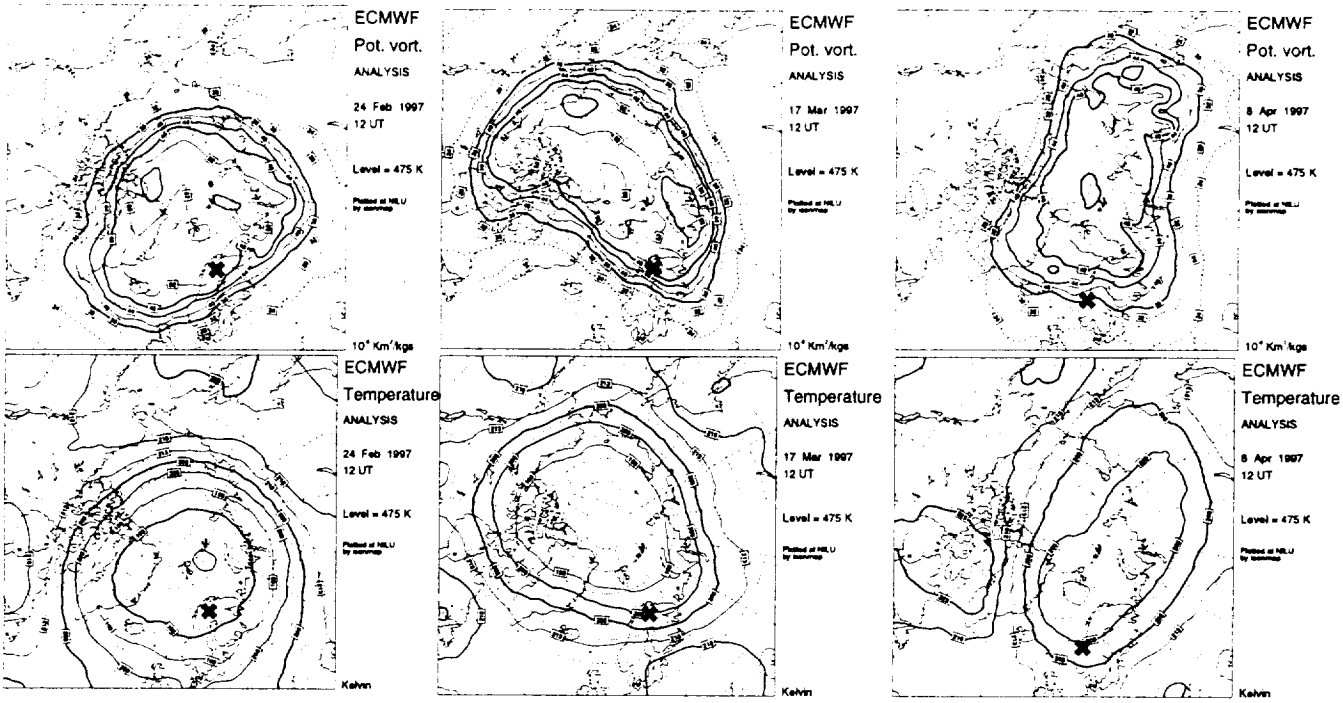
ECMWF
Pot. vort.
ANALYSIS
24 Feb 1997
12 UT
Level = 475 K
10⁻⁶ Km²/kgs
ECMWF
Pot. vort.
ANALYSIS
17 Mar 1997
12 UT
Level = 475 K
10⁻⁶ Km²/kgs
ECMWF
Pot. vort.
ANALYSIS
8 Apr 1997
12 UT
Level = 475 K
10⁻⁶ Km²/kgs
ECMWF
Temperature
ANALYSIS
24 Feb 1997
12 UT
Level = 475 K
Kelvin
ECMWF
Temperature
ANALYSIS
17 Mar 1997
12 UT
Level = 475 K
Kelvin
ECMWF
Temperature
ANALYSIS
8 Apr 1997
12 UT
Level = 475 K
Kelvin

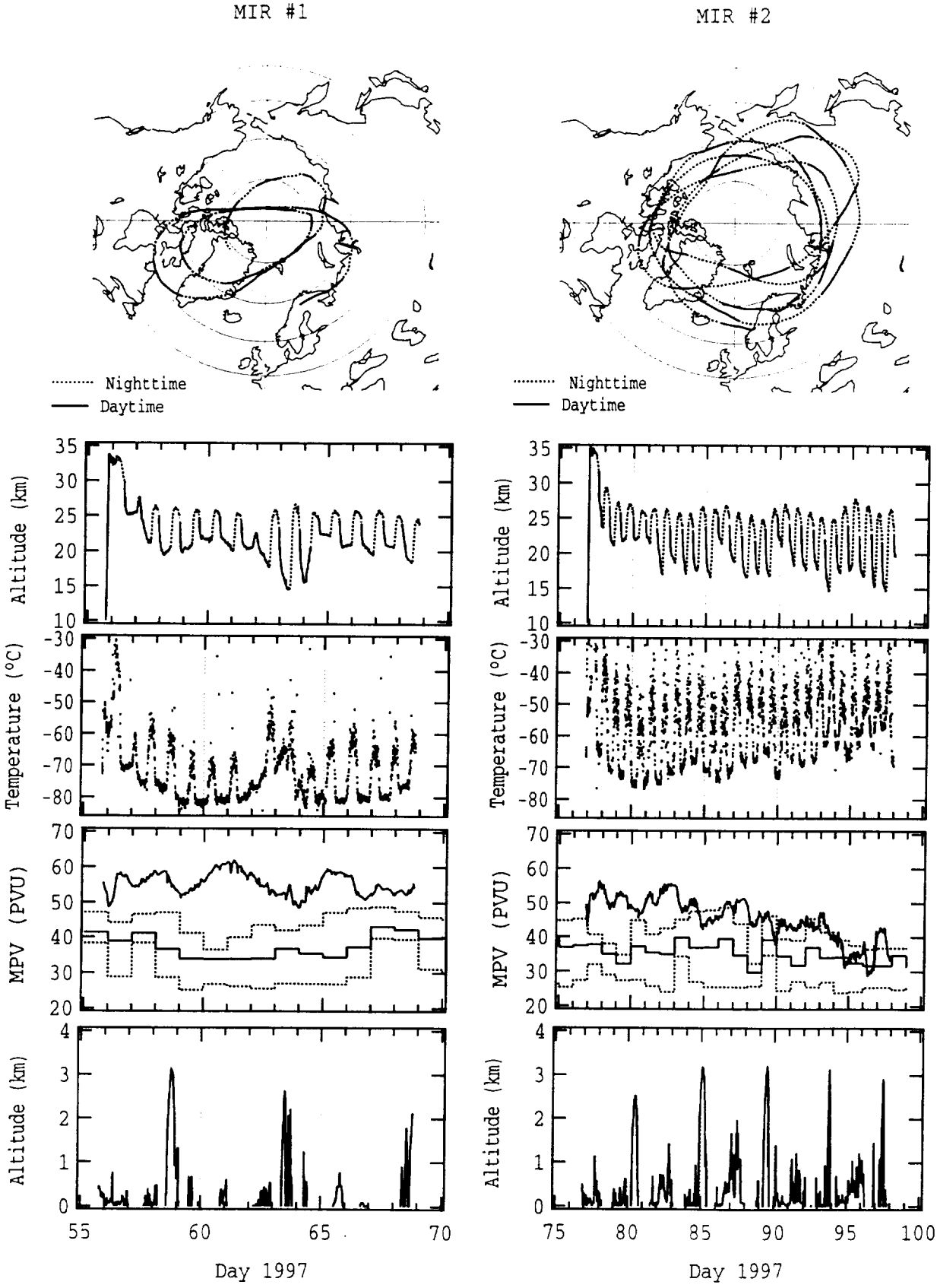
MIR #1
MIR #2
Nighttime
Daytime
Nighttime
Daytime
Altitude (km)
Temperature (°C)
MPV (PVU)
Altitude (km)
Day 1997
Altitude (km)
Temperature (°C)
MPV (PVU)
Altitude (km)
Day 1997

Figure 3

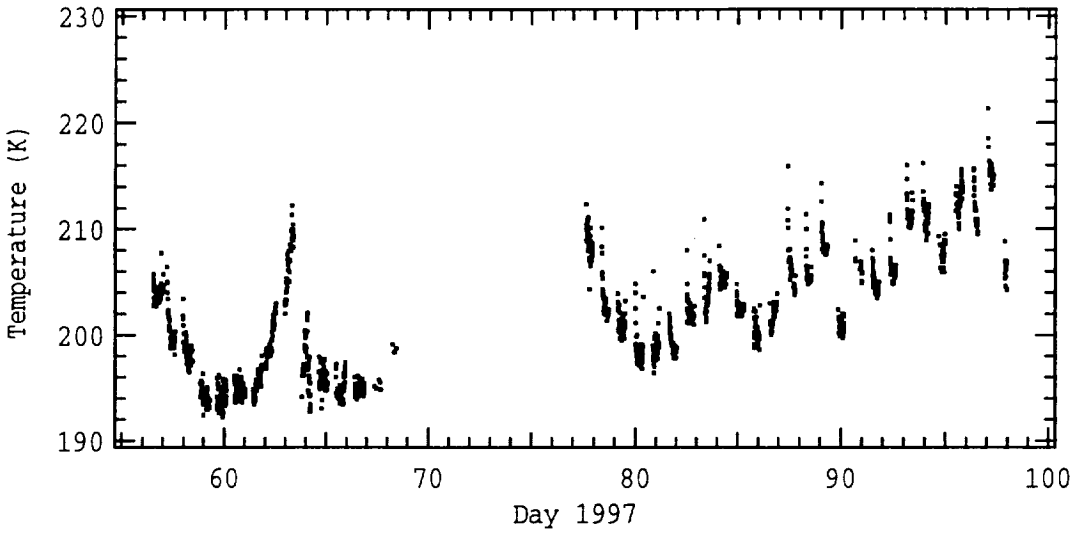
230
220
210
200
190
Temperature (K)
60
70
80
90
100
Day 1997

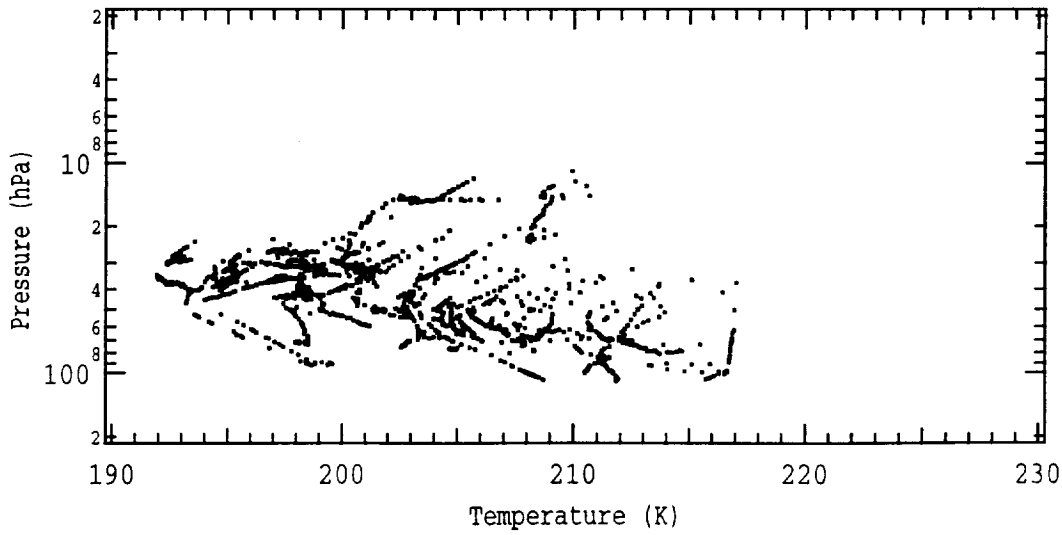
2
4
6
8
10
2
4
6
8
100
2
Pressure (hPa)
190
200
210
220
230
Temperature (K)

Figure 4

Figure 5

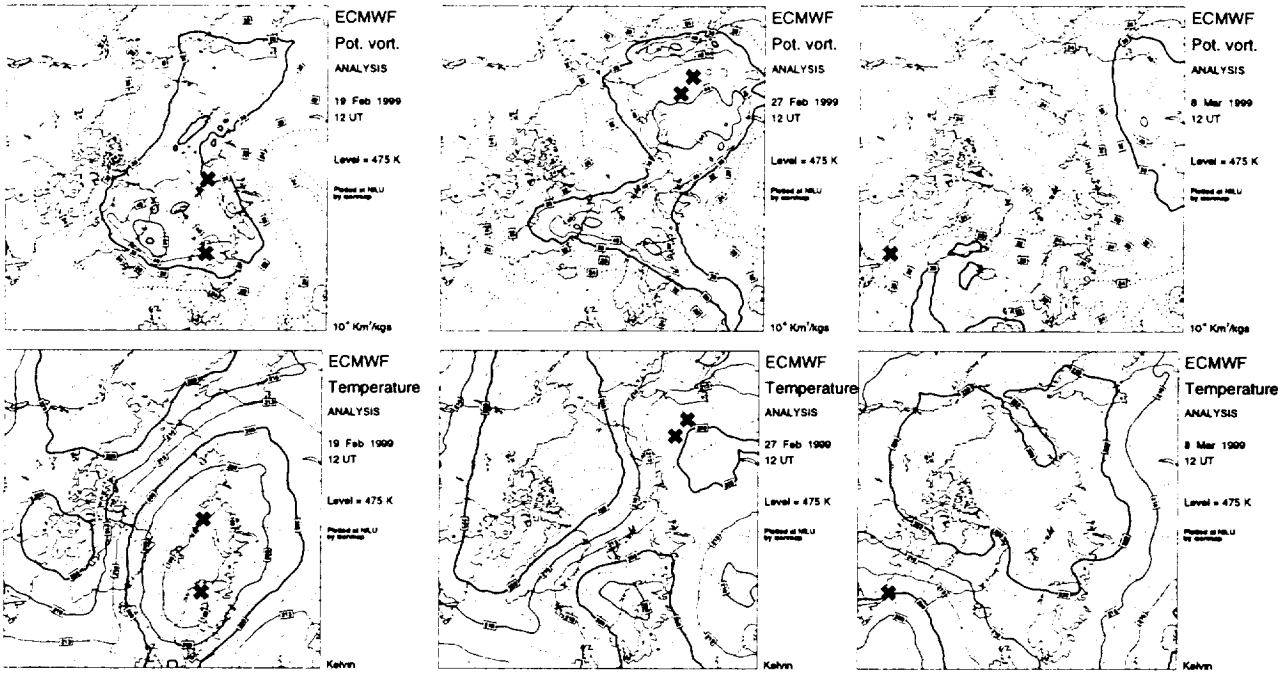
ECMWF
Pot. vort.
ANALYSIS
19 Feb 1999
12 UT
Level = 475 K
10⁻⁶ Km²/kgs
ECMWF
Pot. vort.
ANALYSIS
27 Feb 1999
12 UT
Level = 475 K
10⁻⁶ Km²/kgs
ECMWF
Pot. vort.
ANALYSIS
8 Mar 1999
12 UT
Level = 475 K
10⁻⁶ Km²/kgs
ECMWF
Temperature
ANALYSIS
19 Feb 1999
12 UT
Level = 475 K
Kelvin
ECMWF
Temperature
ANALYSIS
27 Feb 1999
12 UT
Level = 475 K
Kelvin
ECMWF
Temperature
ANALYSIS
8 Mar 1999
12 UT
Level = 475 K
Kelvin

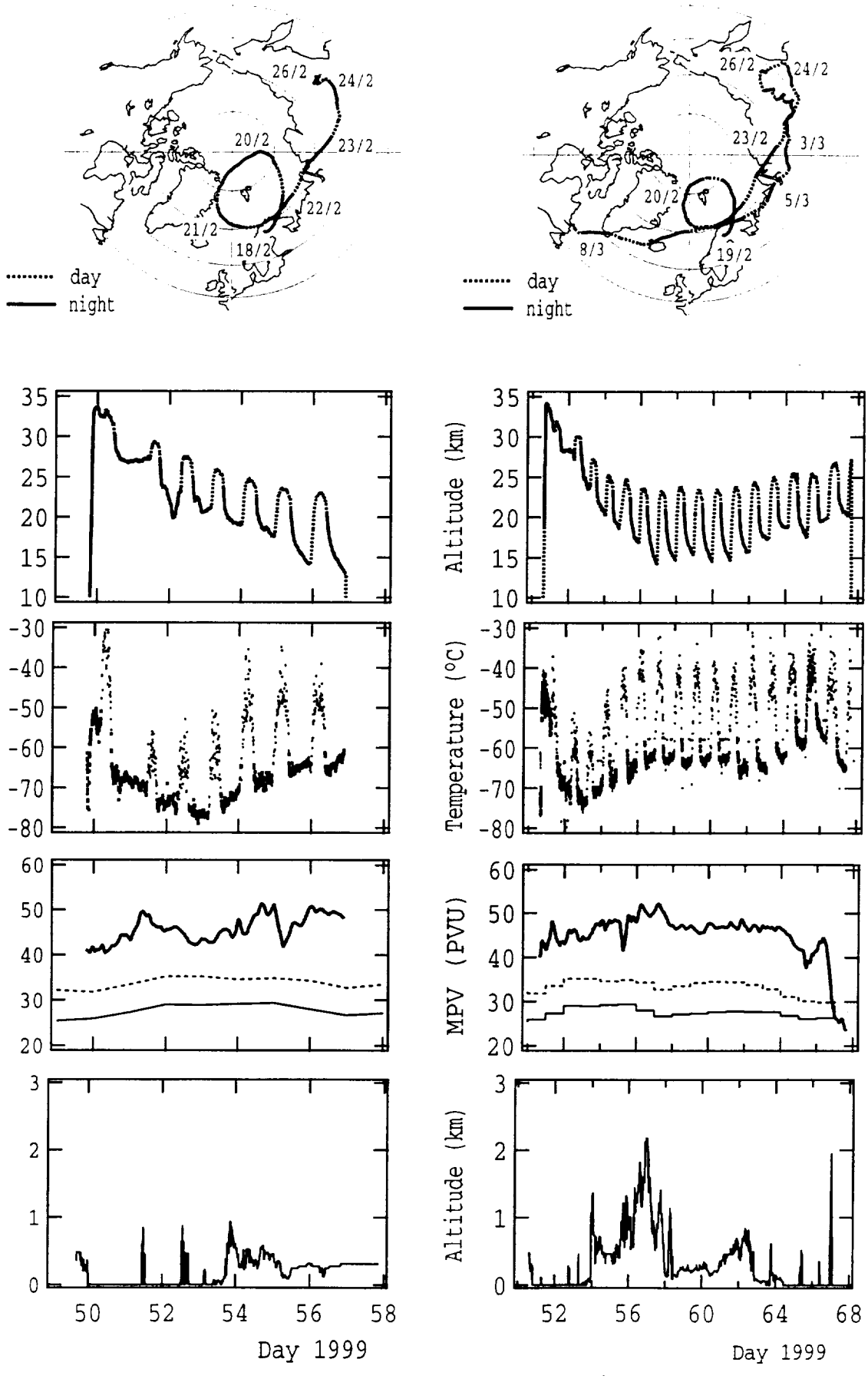
26/2
24/2
20/2
23/2
22/2
21/2
18/2
day
night
26/2
24/2
23/2
3/3
20/2
5/3
8/3
19/2
day
night
Altitude (km)
Temperature (°C)
MPV (PVU)
Altitude (km)
Day 1999
Day 1999

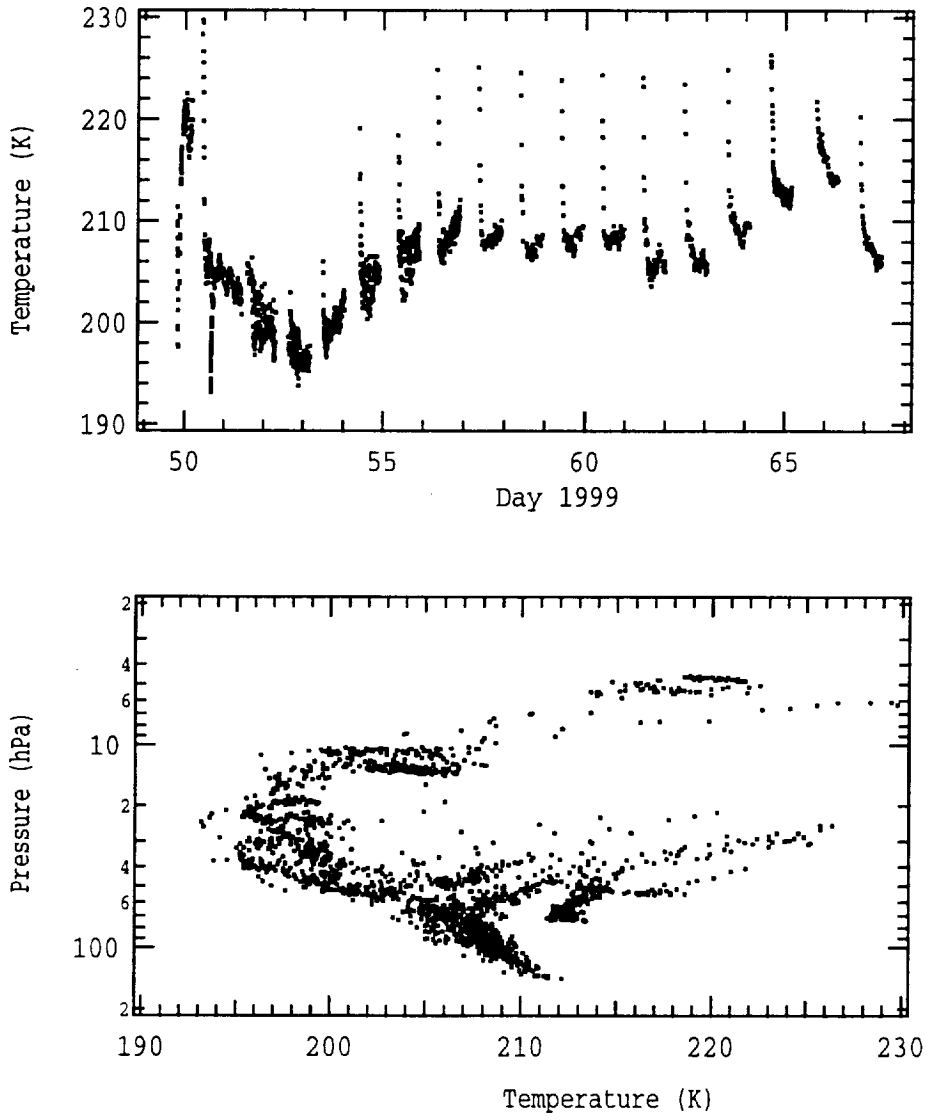
Temperature (K)
230
220
210
200
190
50
55
60
65
Day 1999
Pressure (hPa)
2
4
6
10
2
4
6
100
2
190
200
210
220
230
Temperature (K)

Figure 7

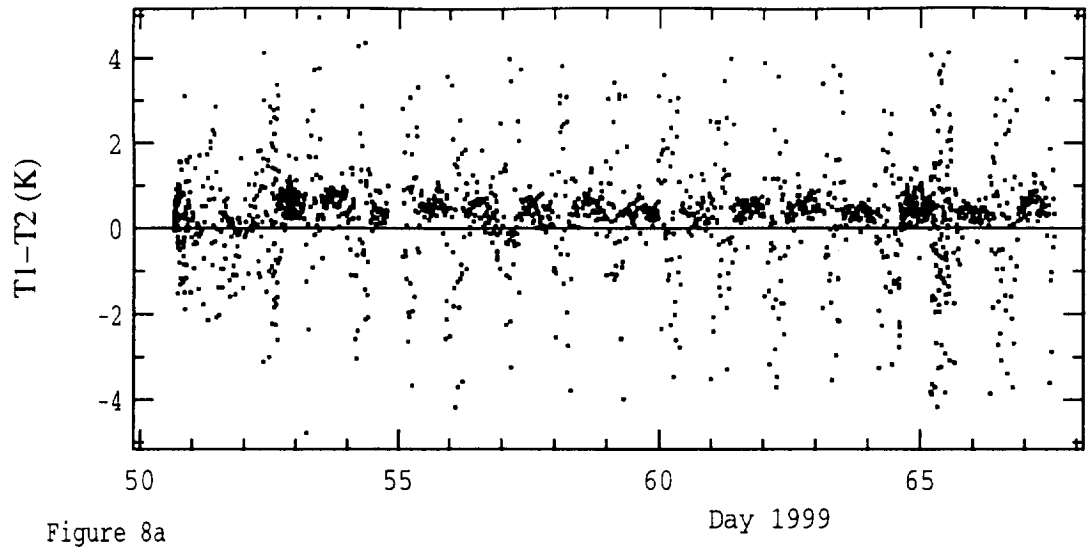

Figure 8a

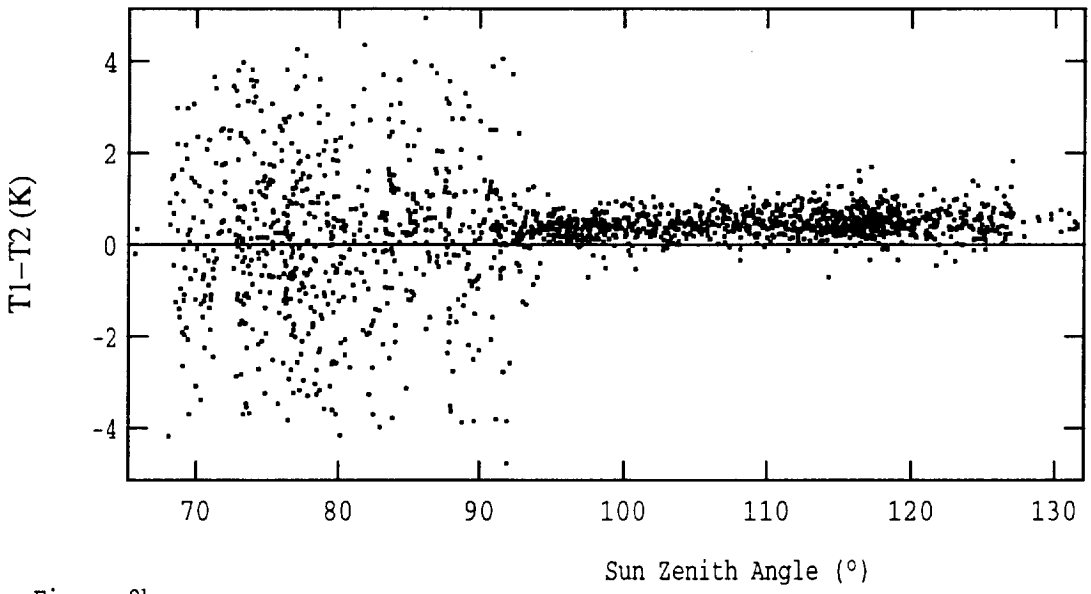

Figure 8b

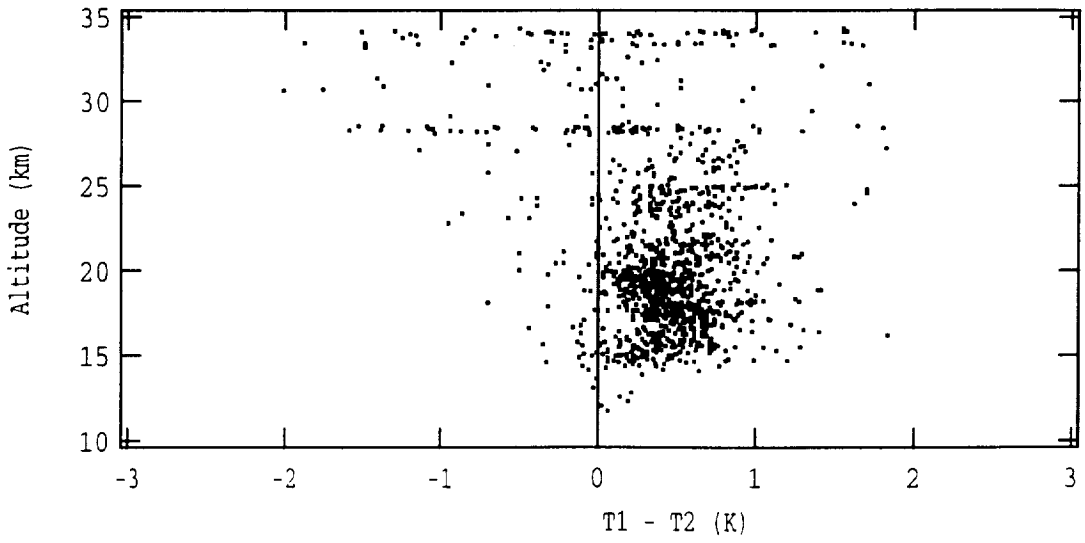

Figure 8c

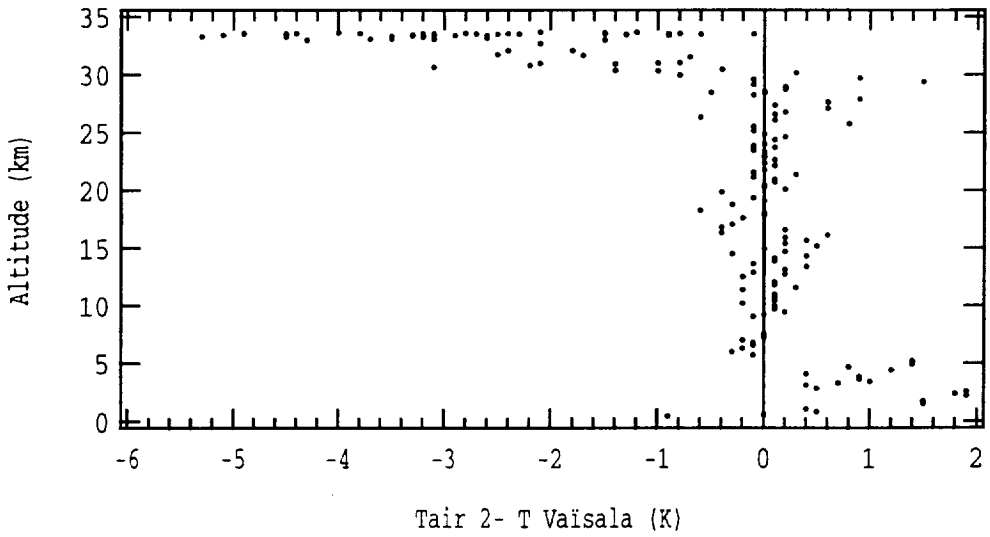

Figure 9

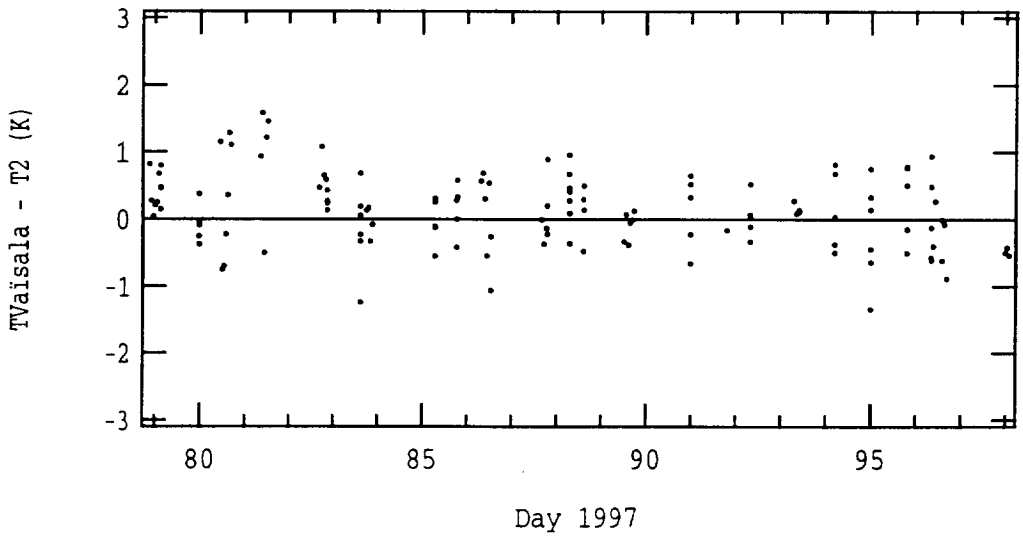

Figure 10

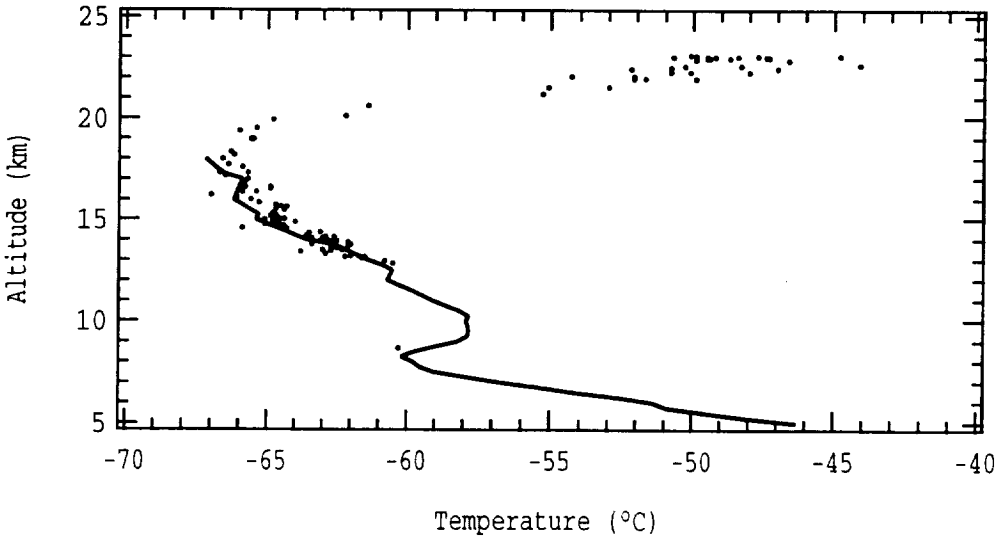

Figure 11